All-optical mode-group multiplexed transmission over a graded-index ring-core fiber with single radial mode

FENG FENG,[1,*] , OXFORD PEOPLE,[2] YONGMIN JUNG,[3] QIONGYUE KANG,[3] PRANABESH BARUA,[3] JAYANTA K. SAHU,[3] SHAIF-UL ALAM,[3] DAVID J. RICHARDSON[3] AND TIMOTHY D. WILKINSON[1]

[1]*Electrical Division, Department of Engineering, University of Cambridge, 9 JJ Thomson Avenue, Cambridge, CB3 0FA, UK*
[2] *University of Oxford, Parks Road, Oxford, OX1 3PJ, UK*
[3]*Optoelectronics Research Centre, University of Southampton, Southampton, SO17 1BJ, UK*
**ff263@cam.ac.uk*

Abstract: A graded-index ring-core fiber (GI-RCF) supporting 3 mode-groups (i.e. LP_{01}, LP_{11} and LP_{21}) with a single radial index of one is designed and fabricated for mode-division multiplexed (MDM) transmission. A spatial light modulator (SLM) is used as a reconfigurable mode (de)multiplexer and spatial/ temporal modal properties of the GI-RCF is systematically characterized. All-optical mode-group multiplexed transmissions is demonstrated over a 360m GI-RCF without using multiple-input multiple-output digital signal processing (MIMO DSP).

OCIS codes: (060.2330) Fiber optics communications; (060.2270) Fiber characterization; (060.4230) Multiplexing.

References and links

1. D. Richardson, J. Fini, and L. Nelson, "Space-division multiplexing in optical fibres," *Nat. Photonics*, vol. 7, no. 5, pp. 354–362, Apr. 2013.
2. R. J. Essiambre, G. Kramer, P. J. Winzer, G. J. Foschini and B. Goebel, "Capacity Limits of Optical Fiber Networks," in *Journal of Lightwave Technology*, vol. 28, no. 4, pp. 662-701, Feb.15, 2010.
3. Guifang Li, Neng Bai, Ningbo Zhao, and Cen Xia, "Space-division multiplexing: the next frontier in optical communication," Adv. Opt. Photon. 6, 413-487 (2014).
4. L. Gruner-Nielsen et al., "Few Mode Transmission Fiber with Low DGD, Low Mode Coupling, and Low Loss," in Journal of Lightwave Technology, vol. 30, no. 23, pp. 3693-3698, Dec.1, 2012.
5. P. Sillard, M. Astruc, D. Boivin, H. Maerten, and L. Provost, "Few-Mode Fiber for Uncoupled Mode-Division Multiplexing Transmissions," in 37th European Conference and Exposition on Optical Communications, OSA Technical Digest (CD) (Optical Society of America, 2011), paper Tu.5.LeCervin.7.
6. G. Labroille, P. Jian, N. Barré, B. Denolle, and J. Morizur, "Mode Selective 10-Mode Multiplexer based on Multi-Plane Light Conversion," in Optical Fiber Communication Conference, OSA Technical Digest (online) (Optical Society of America, 2016), paper Th3E.5.
7. A. M. Velázquez-Benítez et al., "Scaling the Fabrication of Higher Order Photonic Lanterns Using Microstructured Preforms," in ECOC, Spain, 2015, p. Tu.3.3.2.
8. Sun Hyok Chang, Hwan Seok Chung, Nicolas K. Fontaine, Roland Ryf, Kyung Jun Park, Kwangjoon Kim, Jyung Chan Lee, Jong Hyun Lee, Byoung Yoon Kim, and Young Kie Kim, "Mode division multiplexed optical transmission enabled by all–fiber mode multiplexer," Opt. Express 22, 14229-14236 (2014).
9. S. Randel, A. Sierra, S. Mumtaz, A. Tulino, R. Ryf, P. Winzer, C. Schmidt, and R. Essiambre, "Adaptive MIMO signal processing for mode-division multiplexing," in Optical Fiber Communication Conference, OSA Technical Digest (Optical Society of America, 2012), paper OW3D.5.
10. Beril Inan, Bernhard Spinnler, Filipe Ferreira, Dirk van den Borne, Adriana Lobato, Susmita Adhikari, Vincent A. J. M. Sleiffer, Maxim Kuschnerov, Norbert Hanik, and Sander L. Jansen, "DSP complexity of mode-division multiplexed receivers," Opt. Express 20, 10859-10869 (2012).
11. Y. Jung, E. L. Lim, Q. Kang, T. C. May-Smith, N. H. L. Wong, R. Standish, F. Poletti, J. K. Sahu, S. U. Alam, and D. J. Richardson, "Cladding pumped few-mode EDFA for mode division multiplexed transmission," Opt. Express 22, 29008-29013 (2014).
12. E. Ip, M. Li, Y. Huang, A. Tanaka, E. Mateo, W. Wood, J. Hu, Y. Yano, and K. Koreshkov, "146λx6x19-Gbaud Wavelength- and Mode-Division Multiplexed Transmission over 10x50-km Spans of Few-Mode Fiber with a Gain-Equalized Few-Mode EDFA," in Optical Fiber Communication Conference/National Fiber Optic Engineers Conference 2013, OSA Technical Digest (online) (Optical Society of America, 2013), paper PDP5A.2.

13. Q. Kang, E. Lim, Y. Jun, X. Q. Jin, F. P. Payne, S. Alam, and D. J. Richardson, "Gain equalization of a six-mode-group ring core multimode EDFA," presented at the European Conf. Exhibition Optical Communication, Cannes, France, 2014, Paper P.1.14.
14. R. Ryf, N. K. Fontaine, J. Dunayevsky, D. Sinefeld, M. Blau, M. Montoliu, and S. Randel, Chang Liu, Burcu Ercan, M. Esmaeelpour, S. Chandrasekhar, A. H. Gnauck, S. G. Leon-Saval, J. Bland-Hawthorn, J. R. Salazar-Gil, Y. Sun, L. Gruner-Nielsen, R. Lingle, Jr., and D. M. Marom, "Wavelength-Selective Switch for Few-Mode Fiber Transmission," in European Conference and Exposition on Optical Communications, 2013, paper PD1.C.4.
15. Joel Carpenter, Sergio G. Leon-Saval, Joel R. Salazar-Gil, Joss Bland-Hawthorn, Glenn Baxter, Luke Stewart, Steve Frisken, Michaël A. F. Roelens, Benjamin J. Eggleton, and Jochen Schröder, "1x11 few-mode fiber wavelength selective switch using photonic lanterns," Opt. Express 22, 2216-2221 (2014).
16. N. K. Fontaine, R. Ryf, H. Chen, A. V. Benitez, B. Guan, R. Scott, B. Ercan, S. J. B. Yoo, L. E. Grüner-Nielsen, Y. Sun, R. Lingle, E. Antonio-Lopez, and R. Amezcua-Correa, "30×30 MIMO Transmission over 15 Spatial Modes," in Optical Fiber Communication Conference Post Deadline Papers, OSA Technical Digest (online) (Optical Society of America, 2015), paper Th5C.1.
17. P. Sillard, D. Molin, M. Bigot-Astruc, A. Amezcua-Correa, K. de Jongh and F. Achten, "50 µm Multimode Fibers for Mode Division Multiplexing," in Journal of Lightwave Technology, vol. 34, no. 8, pp. 1672-1677, April15, 15 2016.
18. R. Ryf, N. K. Fontaine, B. Guan, B. Huang, M. Esmaeelpour, S. Randel, A. H. Gnauck, S. Chandrasekhar, A. Adamiecki, G. Raybon, R. W. Tkach, R. Shubochkin, Y. Sun, and R. Lingle, Jr., "305-km combined wavelength and mode-multiplexed transmission over conventional graded-index multimode fibre." in Proceedings of European Conference on Optical Communication (2014), paper PD.3.5.
19. G. Labroille, P. Jian, L. Garcia, J. B. Trinel, R. Kassi, L. Bigot, and J.F Morizur, "30 Gbit/s Transmission over 1 km of Conventional Multi-mode Fiber using Mode Group Multiplexing with OOK modulation and direct detection," in the 2015 European Conference and Exhibition on Optical Communication (ECOC), P.5.12.
20. X. Q. Jin, A. Gomez, D. C. O'Brien, and F. P. Payne, "Influence of refractive index profile of ring-core fibres for space division multiplexing systems," in Proc. IEEE Summer Topicals Meeting Series,Montreal, QC, USA, Jul. 2014, pp. 178–179.
21. F. Feng, G. S. Gordon, X. Q. Jin, D. C. O'Brien, F. P. Payne, Y. Jung, Q. Kang, J. K. Sahu, S. U. Alam, D. J. Richardson, and T. D. Wilkinson, "Experimental Characterization of a Graded-Index Ring-Core Fiber Supporting 7 LP Mode Groups," in Optical Fiber Communication Conference, (2015), paper Tu2D.3.
22. F. Feng, X. Guo, G. S. Gordon, X. Jin, F. Payne, Y. Jung, Q. Kang, S. Alam, P. Barua, J. Sahu, D. J. Richardson, I. H. White, and T. D. Wilkinson, "All-optical Mode-Group Division Multiplexing Over a Graded-Index Ring-Core Fiber with Single Radial Mode," in Optical Fiber Communication Conference, OSA Technical Digest (online) (Optical Society of America, 2016), paper W3D.5.
23. Y. Jung; Q. Kang; H. Zhou; R. Zhang; S. Chen; H. Wang; Y. Yang; X. Jin; F. P. Payne; S. u. Alam; D. Richardson, "Low-Loss 25.3km Few-Mode Ring-Core Fiber for Mode-Division Multiplexed Transmission," in Journal of Lightwave Technology, vol.PP, no.99, pp.1-1 (doi: 10.1109/JLT.2017.2658343).
24. C. R. Doerr, N. Fontaine, M. Hirano, T. Sasaki, L. Buhl, and P. Winzer, "Silicon photonic integrated circuit for coupling to a ring-core multimode fiber for space-division multiplexing," in 37th European Conference and Exposition on Optical Communications, (2011), paper Th.13.A.3.
25. Joel Carpenter, Benjamin J. Eggleton, and Jochen Schröder, "110x110 optical mode transfer matrix inversion," Opt. Express 22, 96-101 (2014).
26. Joel Carpenter, Benn C. Thomsen, and Timothy D. Wilkinson, "Degenerate Mode-Group Division Multiplexing," J. Lightwave Technol. 30, 3946-3952 (2012).
27. Xianqing Jin, Ariel Gomez, Kai Shi, Benn C. Thomsen, Feng Feng, George S. D. Gordon, Timothy D. Wilkinson, Yongmin Jung, Qiongyue Kang, Pranabesh Barua, Jayanta Sahu, Shaif-ul Alam, David J. Richardson, Dominic C. O'Brien, and Frank P. Payne, "Mode coupling effects in ring-core fibres for space-division multiplexed systems," J. Lightwave Technol. 34, 3365-3372, 15 July 2016.

1. Introduction

Mode-division multiplexing (MDM) technology, as one embodiment of space-division multiplexing (SDM), has been proposed to substantially increase transmission capacity per fiber by exploiting multiple eigenmodes in a multimode fiber (MMF) as independent data channels [1-3]. For MDM to become a viable solution, several research aspects are very important. For examples, they encompass customized MDM fibers with large (or small) effective index difference between the mode groups for weak (or strong) mode coupling [4,5], spatial mode (de)multiplexers [6-8], multiple-input multiple-output (MIMO) digital signal processing (DSP) to undo mode coupling with low computational complexity [9, 10], as well as multimode counterpart components such as optical amplifiers [11-13] and switches [14,15].

Mode coupling/crosstalk is one of the critical factors to limit overall MDM transmission system performance. In general, MDM transmission with strongly coupled spatial modes requires full mode diversity coherent detection at the receiving end and MIMO DSP. To achieve practical real time operation and reasonable power consumption, reducing receiver computational complexity of MIMO DSP is essential and MIMO optimized MMFs and/or DGD management are employed to lower the complexity of MIMO DSP equalization [17,18]. In long haul transmission application, spatial mode channels over the MDM links are strongly mixed (i.e. strongly coupled regime), MIMO optimized MMFs and/or DGD management are regarded as a promising solution. On the other hand, for short distance supplication such as data center networks, spatial modes/mode-groups are weakly coupled [19] over few kilometer lengths of fiber and direct detection can be applicable without expensive coherent detection and complex MIMO DSP. Therefore, weakly coupled MDM links are very attractive for data capacity upgrade at low cost and low power consumption while reducing cabling footprint in short distance networks. In this paper, a graded-index ring-core fiber (GI-RCF) supporting 3 linearly polarized (LP) mode groups with single radial index was designed and fabricated to achieve relatively weak coupling between all supported spatial mode-groups. Using a reconfigurable spatial light modulator (SLM) based spatial (de)multiplexer, we have experimentally demonstrated 3×12.5Gbit/s and 2×12.5Gbit/s all-optical mode-group multiplexed transmission over a 360m GI-RCF using all guided 3 spatial mode-groups and 2 non-adjacent mode-groups of the GI-RCF with simple on-off keying (OOK) modulation and direct detection. Ring Core Fiber Design and Characterization

2. Ring core fiber design and characterization

2.1 Ring Core Fiber design

RCFs have been reported to be an attractive class of multimode fibers for MDM systems due to their unique features [20-23]. The number of modes supported by a RCF can be adjusted by changing the radius and thickness of the ring layer. To support a relatively large number of guided modes with a large average effective index difference that reduces mode couplings between mode-groups, RCFs are usually designed to support a single radial mode and multiple azimuthal modes. Because of their simpler pattern structures of spatial modes with single radial index, selective ring mode excitation can be performed using a compact silicon photonic integrated circuit with a circular grating coupler fed by an array of waveguides, which has been demonstrated experimentally in [24]. One unique feature that RCFs have is that the propagation constant difference between adjacent mode-groups increase significantly with increasing azimuthal index number of the modes. This feature results in relatively strong coupling between low order mode-groups but weak coupling between high order mode-groups. As a GI-RCF supporting 7 LP mode-groups reported in [21], low order four mode-groups of the fiber are strongly coupled and higher order mode-groups experience relatively weak coupling.

Fig. 1(a)-(c) show the measured refractive index profile of GI-RCF used here, normalized propagation constants of vector modes and theoretical mode filed distributions of all guided LP modes calculated using the refractive index profile. The GI-RCF supports three LP mode-groups with a single radial index of one: LP_{01}, LP_{11} and LP_{21}. Each $LP_{l>0,\,m=1}$ mode has two-fold spatial degeneracy in each polarization, where l and m are the azimuthal and radial index respectively. These sets of degenerate modes form a mode group and mix heavily in the fiber, but mode coupling between mode groups is small.

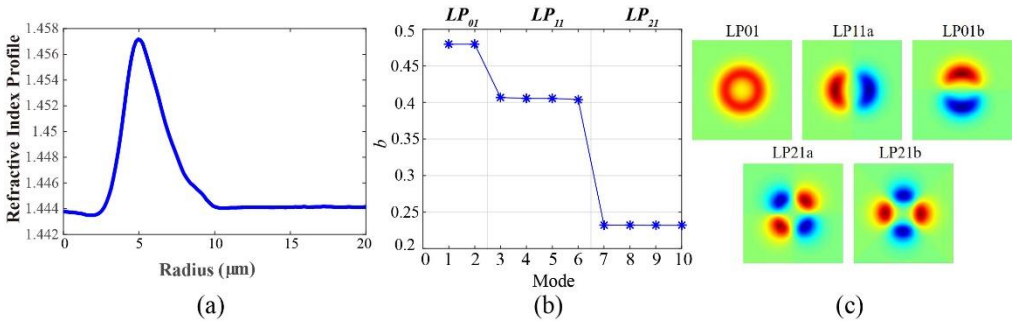

Fig 1. (a) Refractive index profile of the GI RCF, (b) normalized propagation constants of vector modes and (c) theoretical mode field distributions of all guided LP modes in the RCF.

2.2 Experimental Characterization of the GI-RCF

We characterize modal properties of the GI-RCF using precise holographic mode excitation/ detection enabled by reconfigurable SLM based spatial (de)multiplexers. The configuration of SLM based spatial (de)multiplexers is depicted in Fig. 2. Using a polarization diversity configuration, the SLM based spatial (de)multiplexers can accommodate any input polarization state. This configuration also allows launching and detecting each polarization mode individually. Fig. 2 outlines the experimental system used to spatially resolve modal properties of the GI-RCF. We previously employed the system to characterize other RCF designs [21, 22]. Each spatial/polarization mode supported by the GI-RCF is precisely excited and detected by programming corresponding phase masks (holograms) onto the SLM based spatial (de)multiplexers at both ends. The phase masks are generated using simulated annealing algorithm under the constraint of less than 1% error and maximum possible light conversion efficiency in a 70μm radius circle around the fiber core. Fig. 3(b) shows the light conversion efficiency of the generated phase mask that converts a Gaussian beam illumination to each LP mode supported by the GI-RCF with the magnification of the used optical system.

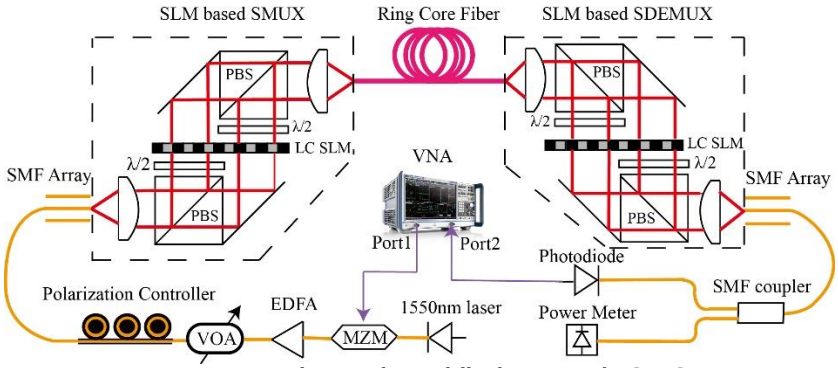

Fig 2. Experimental system that modally characterize the GI-RCF.

SLM based spatial (de)multiplexers support multiple MDM channels. For modal characterization of the fiber, only one channel that maps one input single mode fiber (SMF) port to one output SMF port is used. A polarization controller aligns the input polarization state to ensure it has approximately equal component along horizontal and vertical polarization axes of the system. The multiplexer SLM launches each mode of the GI-RCF in each polarization one at a time. For each mode launch in each polarization, the demultiplexer SLM displays phase masks for each spatial mode in each polarization sequentially to decompose the received modal superposition. A vector network analyzer (VNA) with a frequency range from 40MHz to 20GHz measures frequency/time response for each pair of launch and detect

spatial/polarization modes, producing a full 10×10 mode transfer matrix in the time domain. Fig. 3(a) shows the measured temporal-domain mode transfer matrix aggregated over two launched and detected polarizations. In diagonal elements of the matrix colored in green, single dominant pulses arrive at different time correspond to different propagation modes supported by the GI-RCF. As shown in Fig. 3(c), the measured DGD values was closely matched to the theoretical values calculated from the fiber refractive index profile. From the measured temporal-domain mode transfer matrix, we can separately analyze the mode couplings/crosstalk occurred in the system based on their locations, such as discrete modal crosstalk at spatial multiplexers and distributed mode coupling from the fiber itself.

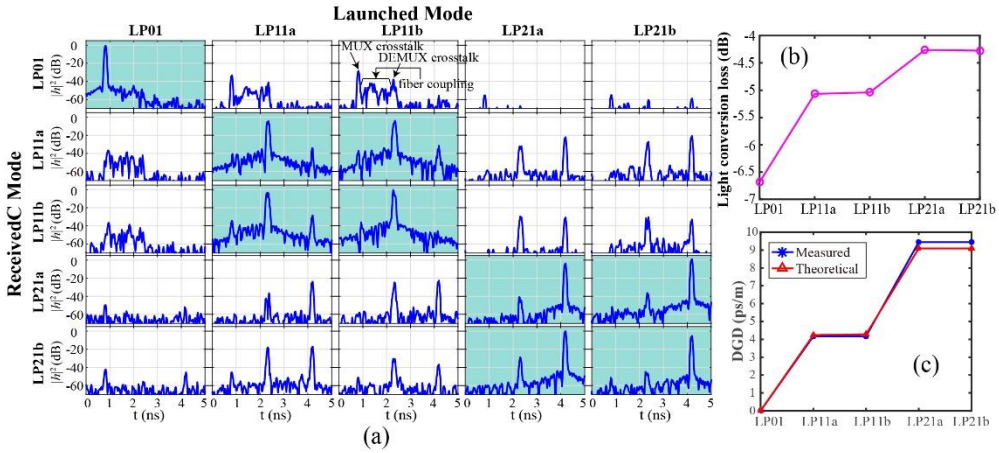

Fig 3. (a) Measured temporal-domain mode transfer matrix (summed over polarizations) of the 360 m GI-RCF. (b) Light conversion loss of the generated phase masks for the LP modes supported by the GI-RCF. (c) Comparison between measured DGDs and designed DGD values of the GI-RCF.

In each cell of the matrix, multiple discrete impulse peaks indicates the modal crosstalk at the spatial (de)multiplexers but energy spread between discrete modal peaks are due to the distributed mode coupling over the length of fibre. For instance, in LP_{01}-LP_{11b} cell of the matrix, a small modal peak detected on the left is a LP_{01} impulse peak as it arrives at the same time with LP_{01} impulse in LP_{01}-LP_{01} cell. This means that when launching LP_{11b}, a small amount of LP_{01} is excited and detected by the spatial demultiplexer receiving LP_{01}. This is a result of cross-coupling from LP_{11} to LP_{01} at the spatial multiplexer. Similarly, a small modal peak on the right in the LP_{01}-LP_{11b} cell is due to crosstalk at the spatial demultiplexer. The energy plateau between the left and right peaks results from distributed mode coupling from the fiber between the two mode groups during the propagation. From the measured temporal-domain mode transfer matrix in Fig 3(a), we can observe that there are relatively strong discrete cross-coupling between LP_{11} and LP_{21} mode-groups at spatial multiplexer and demultiplexer. The maximum crosstalk occurred at spatial multiplexer and at spatial demultipelxer were measured as -13.7dB and -14.5dB respectively. The magnitudes of impulses between the modal peaks resulting from distributed mode-coupling in the GI-RCF are all below -35dB, which indicates distributed mode-coupling from the transmission GI-RCF is much weaker than the discrete modal crosstalk. In the LP_{11}-LP_{11} cells, the slope of the plateau towards to the LP_{21} modal peak is steeper than the slope of the plateau towards to the LP_{01} modal peaks, which suggests that distributed mode-coupling between LP_{01} and LP_{11} is stronger than that between LP_{11} and LP_{21}. This is because of the GI-RCF design whose Δn_{eff} between LP_{01} and LP_{11} mode-groups is smaller than that between LP_{11} and LP_{21} mode-groups and it is also reflected in the DGD measurement shown in Fig. 3(c).

3. All-Optical Mode-Group Division Multiplexing over the GI-RCF

3.1 Mode Channel Characterization

Enabled by reconfigurable SLM based spatial (de)multiplexers, we can characterize optical mode cross-coupling property of each channel that maps one input SMF port to one output SMF port individually by measuring complex mode transfer matrix of each channel with a power meter [25]. During the mode channel characterization, we use a filtered and polarized amplified spontaneous emission source (0.5nm at 1545.54nm) to approximate a high bandwidth channel. The fiber arrays installed at the SLM based spatial (de)multiplexers have seven SMF ports and therefore the SLM based spatial (de)multiplexers support up to seven mode/mode-group channels. We individually measured optical mode transfer matrix of each of all supported channels to study mode-coupling properties between different supported channels. We find that all the channels have nearly identical mode-coupling properties indicated by almost the same power distributions in their mode transfer matrices shown as an example in Fig. 4. This enables us to reroute or add/drop any mode or mode-groups from/to available input/output SMF ports by programing the SLMs due to the identical mode-coupling properties among different channels. In comparison with [22], optical distortions induced by large spacing MOP connectors are much reduced by using SMF arrays with smaller spacing at SLM based spatial (de)multiplexers. Fig. 4 exhibits power distribution of measured optical mode transfer matrix of a typical channel over the 360m GI-RCF. Among all mode channels, modal crosstalk between any adjacent mode-groups is in the range from -14.2dB to -10.6dB and modal crosstalk between two non-adjacent mode-groups is less than -20dB. Relatively weak coupling between mode-groups shown in the mode transfer matrix enables multiplexing and demultiplexing mode-groups all-optically without significant performance penalties.

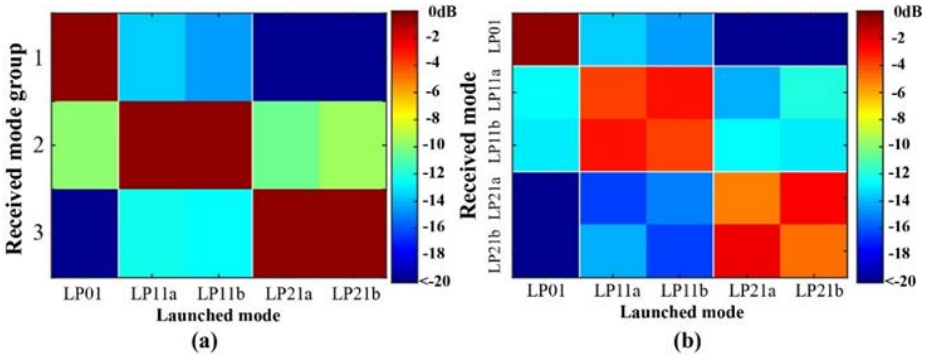

Fig 4. Power distributions (a) aggregated and (b) non-aggregated by mode group of measured optical mode transfer matrix of a typical channel over the 360 m GI-RCF.

3.2 Reconfigurable all-optical mode-group division multiplexing

For the efficient mode (de)multiplexing, multichannel composite phase masks are constructed using the SLM to excite and detect different spatial distributions of modes from/to different input/output SMF ports using a basis library that consists of the phase masks for precisely launching/detecting each mode of the GI-RCF. The multichannel phase mask for one polarization is constructed by superposing phase masks for each individual modal channel and each individual channel's phase mask is a superposition of complex distribution of all constituent modes propagating on that channel and a tilted wavefront that directs the illuminating beam in its corresponding direction with optical aberration correction represented by Zernike polynomials [26]. In this mode-group multiplexing demonstration, independent Gaussian beams with their corresponding incidence angles illuminate the composite phase mask for each polarization at the SLM multiplexer and each Gaussian beam accurately excites a mode in a different mode-group in two polarizations. At the receiving end of the fiber, relative amplitude and phase of all degenerate modes in each of used mode-groups for each polarization are measured first and this information is then used to route the modal distribution of each multiplexed mode-group to its assigned output SMF port. Although the SLM based spatial

(de)multiplexers support polarization division multiplexing (PDM), this work here focus on pure mode-group division multiplexing without combining PDM and polarization diversity information is not measured in the experiments. Two polarization components of each demultiplexed modal channel are combined to the same output SMF port. The phase marks are reconfigurable and can dynamically adjust relative attenuation of each modal channel by assigning an optimized weighting factor to compensate mode dependent loss and equalize received optical power between all modal channels.

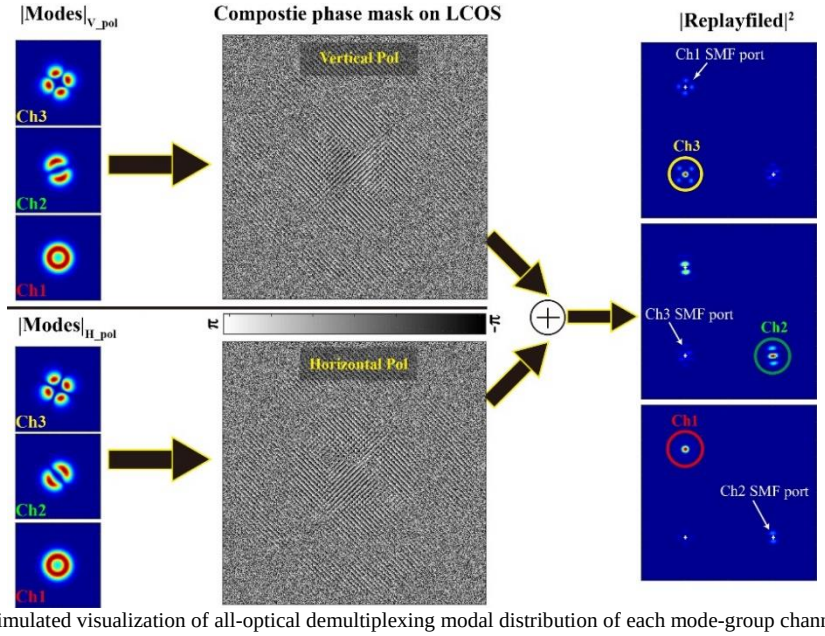

Fig 5. Simulated visualization of all-optical demultiplexing modal distribution of each mode-group channel to its assigned output SMF port in the full (three) mode-group multiplexed transmission experiment over the GI-RCF. White crosshairs show the positions of optical axes of output SMF ports.

Fig. 5 visually illustrates all-optical de-multiplexing operation performed by the SLM based spatial de-multiplexer displaying constructed composite phase masks for two polarizations in the three mode-group multiplexed transmission over the GI-RCF experiment. At the SLM de-multiplexer, launched LP_{01} mode arrives mostly intact with random polarization mixing, whereas launched LP_{11a} or LP_{21a} mode arrives as a random superposition of degenerate modes in each corresponding mode-group with random polarization mixing. The composite phase masks detect the measured modal distributions of each of the three mode-groups in two polarizations and direct them to each assigned output SMF port that corresponds to a spatial position in the replay field. We can see that in the replay field not only do formed autocorrelation peaks (within colored circles in Fig. 5) cover on the target SMF ports but also there are formed cross-correlation distributions surrounding the other channels' output SMF ports. This results from superposing phase masks of each channel to construct the multichannel composite phase mask and there is a loss associated with the superposition. We also observe that the intensities of the formed cross-correlation distributions near the LP_{01} (Ch1) and LP_{11} (Ch2) output SMF ports are relatively stronger when respectively demultiplexing LP_{11} and LP_{01} mode-groups, which indicates relatively higher splitting loss. This is because there is a relatively big intensity overlap between LP_{01} and LP_{11} mode of the GI-RCF. LP_{21} mode that propagates much closer to the outer cladding of the GI-RCF has small intensity overlaps with LP_{01} and LP_{11} mode that propagate near the inner cladding of the GI-RCF. Therefore, the multichannel composite phase mask performs a more efficient split between LP_{21} and the other modes. The intensity diversity between the modes can also be observed from the structure of

the composite phase mask, the inner, middle and outer region of which are respectively of the form of the LP_{01}, LP_{11}, and LP_{21} phase masks.

3.3 Data transmission performance

The experimental system used for the data transmission test is shown in Fig. 6. It is comprised of the transmitter, SLM based spatial (de)multiplexers, the transmission GI-RCF and the receiver. An Anritsu MP1800A bit error rate tester (BERT) was used for both pulse pattern generation and error detection. A Mach-Zehnder modulator driven by the BERT modulates a 1550 nm laser to generate a 12.5Gbps non-return-to-zero (NRZ) 2^{31}-1 pseudo random binary sequence (PRBS) data pattern. The signal is then split into three tributaries that are decorrelated with large relative delays. These three decorrelated signals are accurately launched into the LP_{01}, LP_{11a} and LP_{21a} mode of the GI-RCF. After transmission over the 360m GI-RCF, the SLM de-multiplexer measures complex coefficients of all degenerate modes in each of the three mode-groups in each polarization given the mode launch and uses this information to construct three-channel composite phase masks to demultiplex each mode-group channel to its desired output SMF port. The weighting of each channel in the composite phase mask is optimized through an iterative feedback algorithm to equalize received optical power and minimize crosstalk between channels. A photo-detector connected back to the BERT system was used to sequentially measure the BER performance of each channel as a function of the received optical power.

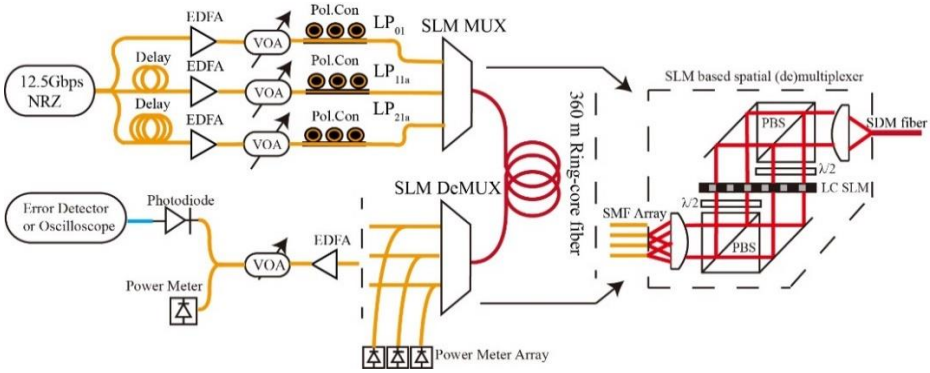

Fig 6. Mode-group division multiplexing system that optically multiplexes three spatial mode-groups from separate input SMF ports into the GI-RCF and de-multiplexes the mode-group channels to separate output SMF ports.

We performed two sets of mode-group division multiplexing over the GI-RCF: three mode-group multiplexed transmission using all supported mode-groups and two mode-group multiplexed transmission using the two non-adjacent mode-groups. Fig. 7 presents measured BER performance as a function of the received optical power for these experiments. In the three mode-group multiplexing experiment, the measured overall optical leakage to each channel from the other two channels was -12.6dB at the start of the BER measurements. We achieve BER below the hard-decision forward error correction (FEC) threshold (3.8×10^{-3}) for the three mode-group multiplexed channels and the required power penalty at the FEC threshold were 1.8dB over single-channel operation for all three channels because of residual crosstalk between mode-group channels. In these two mode-group multiplexing experiments, the optical path for LP_{11a} was disconnected from the system shown in Fig. 6 and the reconfigurable SLM based spatial (de)multiplexers are programed with two-channel composite phase masks at both ends for multiplexing and demultiplexing the two mode-group channels. The optical isolation between the two modal channels were measured as 20dB. Error free (BER<10^{-12}) data transmission was achieved in the two mode-group multiplexing experiment. The two mode-

group multiplexing operation suffers 1.1dB power penalty over single channel operation at a BER of 10^{-12}.

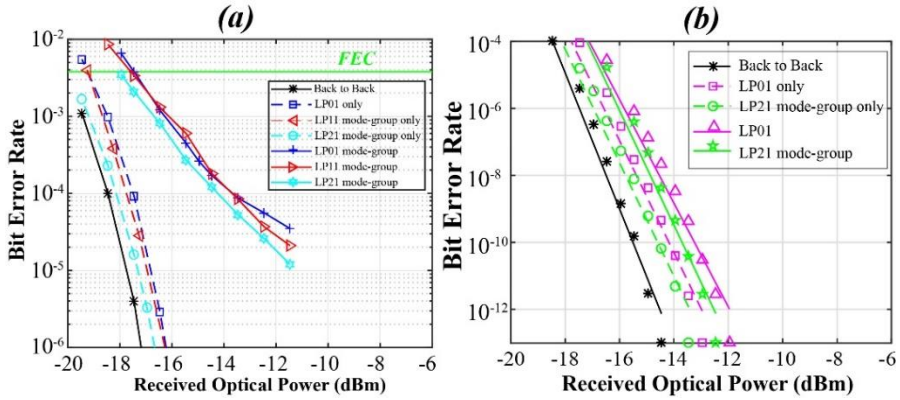

Fig 7. Measured BER curves versus received optical power at 12.5Gbps NRZ: (a) three mode-group multiplexed transmission over the GI-RCF using all supported mode-groups, and (b) two mode-group multiplexed transmission using the two non-adjacent mode-groups.

4. Conclusion

Using a reconfigurable SLM based spatial (de)multiplexer, we have successfully demonstrated all-optical mode-group multiplexed transmissions over a customized 360m graded-index ring-core fiber supporting 3 LP mode-groups without MIMO processing. Weak coupling between mode-groups enables us to achieve BER far below the FEC threshold in three mode-group multiplexed transmission (3×12.5Gbps NRZ) and error free (BER<10^{-12}) in two mode-group multiplexed transmission (2×12.5Gbps NRZ). Resultant power penalties over single channel operations were respectively 1.8dB at the FEC threshold for the 3 mode-group multiplexing and 1.1dB at a BER of 10^{-12} for the 2 mode-group multiplexing. Detailed modal cross-coupling properties of the customized graded-index ring-core fiber are also characterized by measuring complex mode transfer matrix.

Acknowledgements

This works was supported by the UK EPSRC grant: EP/J009369/1 (COMIMO).